Proc. Natl. Acad. Sci. USA
Vol. 95, pp. 15362–15367, December 1998
Cell Biology

The Arp2/3 complex mediates actin polymerization induced by the small GTP-binding protein Cdc42

LE MA, RAJAT ROHATGI, AND MARC W. KIRSCHNER*

Department of Cell Biology, Harvard Medical School, Boston, MA 0211

Contributed by Marc W. Kirschner, October 19, 1998

ABSTRACT **The small GTP-binding protein Cdc42 is thought to induce filopodium formation by regulating actin polymerization at the cell cortex. Although several Cdc42-binding proteins have been identified and some of them have been implicated in filopodium formation, the precise role of Cdc42 in modulating actin polymerization has not been defined. To understand the biochemical pathways that link Cdc42 to the actin cytoskeleton, we have reconstituted Cdc42-induced actin polymerization in *Xenopus* egg extracts. Using this cell-free system, we have developed a rapid and specific assay that has allowed us to fractionate the extract and isolate factors involved in this activity. We report here that at least two biochemically distinct components are required, based on their chromatographic behavior and affinity for Cdc42. One component is purified to homogeneity and is identified as the Arp2/3 complex, a protein complex that has been shown to nucleate actin polymerization. However, the purified complex alone is not sufficient to mediate the activity; a second component that binds Cdc42 directly and mediates the interaction between Cdc42 and the complex also is required. These results establish an important link between a signaling molecule, Cdc42, and a complex that can directly modulate actin networks *in vitro*. We propose that activation of the Arp2/3 complex by Cdc42 and other signaling molecules plays a central role in stimulating actin polymerization at the cell surface.**

Actin polymerization is essential to many dynamic cellular processes, such as the formation of protrusive structures in motile cells, and is highly regulated by spatial and temporal signals. A family of signaling molecules, the Rho-like small GTP-binding proteins, have been implicated in controlling actin polymerization because they are involved in many actin-dependent processes (1). One member, Cdc42, has been shown to regulate filopodial extension (2, 3), cell polarity (4, 5), and cytokinesis (6). To understand the mechanism by which Cdc42 regulates actin polymerization in these processes, an enormous effort has been focused on the identification of proteins that interact with Cdc42. By using affinity chromatography or yeast two-hybrid selection, many Cdc42 target proteins have been found, including PAK (7), ACK (8), Gek (9), and the Wiskott–Aldrich syndrome protein (10). Although some of these proteins have been shown to modulate Cdc42-induced cellular responses (11), the precise role of Cdc42 in regulating actin polymerization has not been defined.

To examine these complex processes biochemically, several groups, including ours, have reconstituted Cdc42-induced actin polymerization in cell-free systems (12, 13). Using *Xenopus* egg extracts, we developed a rapid and specific assay for this activity and attempted to isolate factors involved. After fractionating the extract, we found that at least two biochemically distinct components were required for the activity. By conventional protein purification, we identified one component as the Arp2/3 complex, a protein complex that nucleates actin polymerization (14). However, the Arp2/3 complex alone is not sufficient to mediate the activity; a second component that binds Cdc42 directly and mediates the interaction between Cdc42 and the complex also is required. These results established a regulatory pathway that connects a signaling molecule and a complex that directly modulates actin filament assembly *in vitro* (14). Because recent studies have implicated that the nucleation activity of the Arp2/3 complex might be regulated in cells (14, 15), our findings suggest a role for Cdc42 in the recruitment and activation of the complex and the subsequent stimulation of actin polymerization at the cell surface.

MATERIALS AND METHODS

Preparation of Recombinant G Proteins and *Xenopus* Egg Extracts. Baculorviruses containing coding regions of Cdc42, Rac1, or RhoA fused with glutathione *S*-transferase (GST) at their N termini (kindly provided by Kimberly Tolias and Christopher Carpenter, Beth Israel Hospital, Boston) were used to infect Sf9 cells at a density of 1×10^6 cells/ml. Seventy-two hours after infection, cells were harvested, and recombinant GST-fusion proteins were purified by using glutathione-Sepharose beads (Pharmacia) and were charged with guanosine 5′-[γ-thio]triphosphate (GTPγS) or guanosine 5′-[β-thio]diphosphate (GDPβS) as described (13). High speed supernatants of *Xenopus* egg extracts were prepared as before in XB (10 mM Hepes, pH 7.7/100 mM KCl/2 mM $MgCl_2$/0.1 mM $CaCl_2$/5 mM EGTA/1 mM DTT) (13).

Functional Visual Assay for Cdc42-Induced Actin Polymerization in Extracts. All reactions were carried out at room temperature unless otherwise specified. Seven microliters of reaction mixture containing high speed supernatants (6 μl) or column fractions in XB were supplemented with rhodamine-labeled actin (1 μM for high speed supernatants or 2.5 μM for column fractions) and an energy regenerating mix (16). Glutathione Sepharose beads (1 μl, 50% slurry) bound with 1–2 mg/ml GST-fusions of GTP-binding proteins then were added to start the reaction. Five microliters of the reaction mix was squashed between two glass coverslips and was viewed under a fluorescence microscope (13) at different time points. Activities were estimated visually based on the intensity of rhodamine signal around the beads on a six-unit scale. Images presented in the figures were taken 10–20 minutes after incubation.

Pyrene Actin Assay. The assay was carried out in a total volume of 80 μl of XB. The reaction mix contained high speed supernatants (20 μl) or column fractions (20 μl each), pyrene-

The publication costs of this article were defrayed in part by page charge payment. This article must therefore be hereby marked "*advertisement*" in accordance with 18 U.S.C. §1734 solely to indicate this fact.

Abbreviations: MCAP, mediator of Cdc42-induced actin polymerization; GST, glutathione *S*-transferase; GTPγS, guanosine 5′-[γ-thio]triphosphate; GDPβS, guanosine 5′-[β-thio]diphosphate.

*To whom reprint requests should be addressed at: Department of Cell Biology, Harvard Medical School, 240 Longwood Avenue, Boston, MA 02115. e-mail: marc@hms.harvard.edu.

labeled G-actin (1 μM), and an energy regenerating mix. It was monitored in a fluorometer (13) for 5 minutes to make sure the baseline was stable. GTP-binding proteins then were added. To avoid light scattering from the beads, GTP-binding proteins used here were eluted by digesting GST-fusion proteins with thrombin (CalBiochem, 2 units/100 ng protein substrates) on glutathione beads overnight (17) and taking the supernatant.

Fractionation of High Speed Supernatants on an Anion Exchange Column. All column chromatography described here and below was performed at 4°C on a fast protein liquid chromatography system using columns and media from Pharmacia. Diluted high speed supernatants (2 mg/ml) were loaded to a Resource Q column equilibrated with XB. The flow through was collected, and bound proteins were eluted with 0.5 M extra KCl. Both fractions were concentrated in centriprep-10 (Amicon), were desalted on PD-10 columns (Pharmacia) equilibrated with XB, and were reconcentrated to 50% of the original volume. Three microliters of each fraction then was used in the visual assay.

Assay for Mediator of Cdc42-Induced Actin Polymerization (MCAP). Because both the flowthrough and eluate fractions from the Resource Q column are required for Cdc42-induced actin polymerization, we will refer to the activity in the flow-through as MCAP1 and the activity in the eluate as MCAP2. To assay for MCAP1, an MCAP2-containing fraction (3 μl) was mixed with each column fraction in the visual assay as described above. The MCAP2-containing fraction was prepared from high speed supernatants, which were fractionated sequentially by ammonium sulfate precipitation (40%) and Resource Q chromatography (pH 8.0). This Q-bound fraction contains MCAP2 and is functionally equivalent to the Resource Q eluate fractionated directly from high speed supernatants.

Purification of MCAP1. To purify MCAP1, the flow through from the Resource Q fraction first was precipitated with ammonium sulfate between 43 and 58%. The precipitate was resuspended in a buffer (50 mM potassium phosphate, pH 7.3/30% ammonium sulfate/1 mM DTT) and was loaded on a Resource Phenyl column. The activity bound to the column was eluted with a linear decreasing ammonium sulfate gradient. Active fractions eluted at 15% ammonium sulfate were identified, pooled, and precipitated with 65% ammonium sulfate. The protein pellet then was resuspended and dialyzed into buffer S (9 mM K-Pipes, pH 6.8/30 mM KCl/1 mM DTT) and was loaded on a Mono S column equilibrated with buffer S. About 14% of total protein bound to the Mono S column and MCAP1 eluted immediately after a major protein peak at ≈100 mM KCl. Peak fractions were pooled and separated on a Superdex-75 gel filtration column equilibrated with buffer Q (10 mM Tris·HCl, pH 7.5/100 mM KCl/1 mM DTT). The active fraction then was adjusted to pH 8.8 and was refractionated on a Mono Q column equilibrated with buffer Q (pH 8.8). The activity eluted between 90 and 145 mM KCl.

Assays for Cdc42 Interaction with MCAPs or the Arp2/3 Complex. For the depletion assay, 40 μl of the flow through (MCAP1) or the eluate (MCAP2) from the Resource Q column was mixed with glutathione-Sepharose beads bound with GTPγS- or GDPβS-charged GST-Cdc42 (15 μl of packed beads, 10 μg/μl Cdc42) made from bacteria. After incubation at 4°C for 40 minutes, beads were pelleted, and 20 μl of the supernatant was taken in the functional assays. For the spin down assay, 2 μl of packed beads containing GST-Cdc42-GTPγS (1.4 mg/ml, purified from Sf9 cells) were incubated with the flow through and the eluate (15 μl each) or XB for 5 or 10 minutes and then were washed three times with XB. Bound proteins (precipitated from 11 μl of flow through) were analyzed by immunoblotting with antibodies against Arp3. The flow through and the eluate (0.5 μl each) were loaded as controls.

RESULTS

A Functional Visual Assay for Cdc42-Induced Actin Assembly. We developed a visual assay for Cdc42-induced actin polymerization in the high speed supernatant of *Xenopus* egg extracts. Rhodamine-labeled actin was added to the supernatant to allow visualization of actin polymerization by fluorescence microscopy (13). When glutathione-Sepharose beads coated with GTPγS-charged GST-Cdc42 were added to the high speed supernatant, actin filaments accumulated around beads in the form of punctate foci. The formation of foci required the extract and could be inhibited by cytochalasin D, a drug that blocks filament formation. With time, the number of foci increased until bright haloes of actin formed around each bead at ≈3 minutes (Fig. 1*a*). Some foci seemed to leave the beads and float into the extract, possibly because of the endogenous glutathione that eluted GST-Cdc42 from the beads. A closer examination of the actin foci near the bead periphery under higher magnification revealed that they contained elongated structures (Fig. 1*b*), some of which resembled the comet tails induced by *Listeria monocytogenes* (18, 19). The

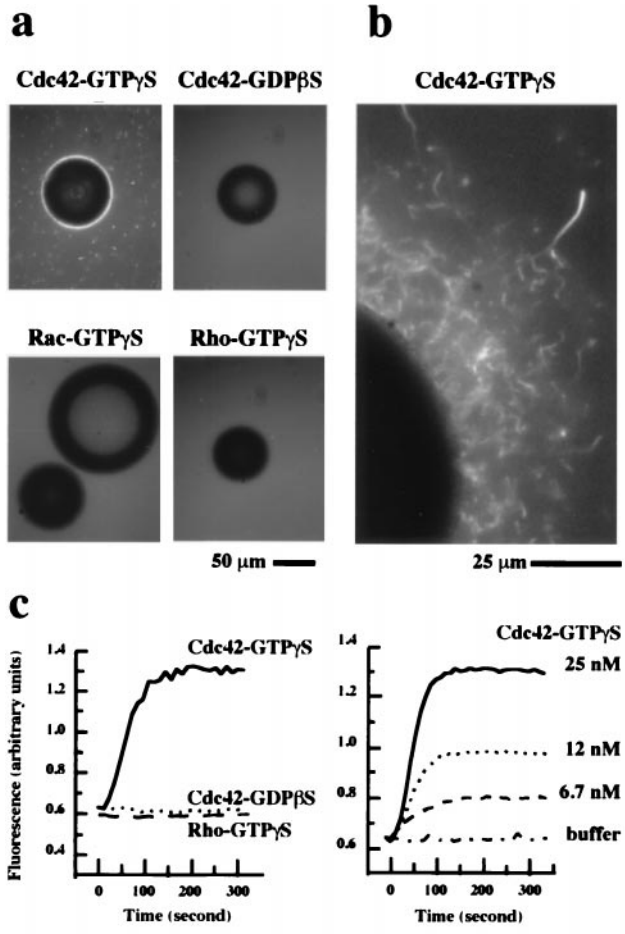

FIG. 1. Assays for Cdc42-induced actin polymerization in *Xenopus* high speed supernatants. (*a*) Actin polymerization was monitored by the visual assay in which rhodamine actin (1 μM) was used to follow actin polymerization by fluorescence microscopy. The extracts were stimulated with glutathione Sepharose beads coated with GST-Cdc42, GST-Rac, or GST-Rho (2 mg of protein/ml packed beads) charged with GTPγS or GDPβS. Bright fluorescence around the bead indicated polymerized actin. (*b*) A high magnification view of actin polymerization around a bead coated with GST-Cdc42-GTPγS. (*c*) Kinetics of actin polymerization in high speed supernatants as monitored by the pyrene actin assay in which fluorescence increase indicates the formation of actin filaments. Extracts were stimulated by Cdc42-GTPγS (25 nM), Cdc42-GDPβS (25 nM), and Rho-GTPγS (50 nM) (left) or by Cdc42-GTPγS at different concentrations (right).

visual assay is only semiquantitative because the extent of actin polymerization is estimated based on the fluorescence intensity around the beads. To follow the polymerization kinetics more quantitatively and to confirm the visual results, we tested the activity of Cdc42 in a pyrene actin assay in which actin polymerization was monitored in a fluorometer. Addition of GTPγS-charged Cdc42 (25 nM) to the extract resulted in a rapid fluorescence increase, an indicator of filament formation (Fig. 1*c*). A new steady state was reached by 5 minutes when ≈10% of the total actin was polymerized (as compared with total fluorescence signal in the presence of phalloidin, a drug that drives all of the actin into polymers).

Actin polymerization in this visual assay is specific for Cdc42 (Fig. 1*a*), as confirmed by the pyrene actin assay (Fig. 1*c*). Rac and Rho, two other members in the Rho family of small GTP-binding proteins, failed to induce actin polymerization in the high speed supernatant (Fig. 1 *a* and *c*). Actin polymerization also depends on the nucleotide bound to Cdc42: GTPγS-charged Cdc42 was active, but GDPβS-charged Cdc42 was not (Fig. 1 *a* and *c*). In addition, actin polymerization seems to require prenylated Cdc42 because only Cdc42 expressed in Sf9 cells and purified from the membrane fraction stimulated the activity. Neither wild-type Cdc42 expressed in and purified from bacteria, presumably without any lipid modification, nor a mutant Cdc42 lacking the C-terminal prenylation site could function in the visual assay (data not shown). Finally, the activity is sensitive to the amount of GST-Cdc42 on the beads (data not shown). This is confirmed by the pyrene actin assay in which both the rate of actin polymerization and the total polymer mass depended on the Cdc42 concentration (Fig. 1*c*). These results demonstrate that actin polymerization observed in this visual assay shares the same characteristics as that described previously in extracts from neutrophils (12) and *Xenopus* eggs (13).

Two Biochemically Distinct Activities Are Required for Cdc42-Induced Actin Polymerization. Using this rapid and sensitive visual assay, we fractionated the high speed supernatant to identify components that allow Cdc42 to stimulate actin polymerization in extracts. We first passed the supernatant over an anion exchange column (Resource Q) at pH 7.7 and tested the activity of the flow through or the eluate fraction. Neither fraction alone induced any actin polymerization in response to Cdc42; the activity seen in the high speed supernatant was recovered only when both fractions were combined (Fig. 2 *a* and *b*). In the following text, we will refer to the activity in the flow through as MCAP1 and the activity in the eluate as MCAP2.

We estimated the apparent molecular weights of MCAP1 and MCAP2 by Superose-6 gel filtration chromatography. Based on their complementing activity, MCAP1 eluted at 210 kDa whereas MCAP2 eluted at 400–500 kDa (data not shown). We also performed affinity-depletion experiments to determine their affinities for Cdc42. The fraction containing MCAP1 was first incubated with GST-Cdc42-GTPγS-beads. After the beads were spun out, the supernatant was tested in the presence of MCAP2, and full activity of MCAP1 was retained in both the visual and pyrene actin assays (Fig. 2 *c* and *d*). However, the activity was lost in the reciprocal experiment in which the depleted supernatant from the MCAP2 fraction was mixed with MCAP1 (Fig. 2 *c* and *d*). Thus, Cdc42 depletes only MCAP2 but not MCAP1. Moreover, the depletion occurred only when GTPγS-charged Cdc42 was used (Fig. 2 *c* and *d*). Of interest, when the beads exposed to MCAP2 were washed and examined in the presence of MCAP1, they assembled actin filaments (data not shown), indicating that MCAP2 bound to the beads was functional. Taken together, these results suggest that MCAP2 and MCAP1 are distinct from each other.

Purification of the Arp2/3 Complex as MCAP1. To identify the MCAP1 activity, we further fractionated the Resource Q

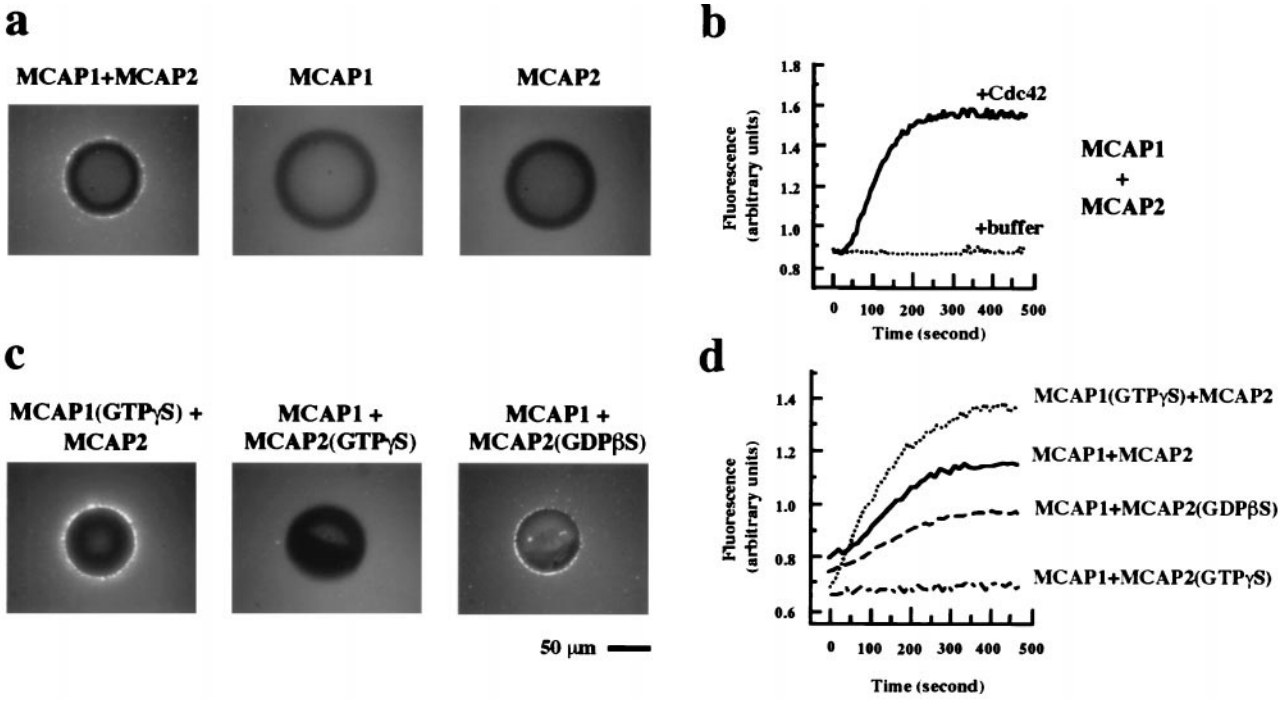

FIG. 2. Two distinct components are found in *Xenopus* extracts that are both required for Cdc42-induced actin polymerization. (*a*) Actin polymerization induced by Cdc42 in reactions containing MCAP1 or MCAP2 or both. (*b*) The time course of actin polymerization induced by Cdc42 or buffer by using combined MCAP1 and MCAP2 fractions (20 μl each). (*c* and *d*) Depletion of MCAP2 but not MCAP1 by Cdc42. Actin polymerization was assayed in fractions depleted by beads coated with GST-Cdc42 charged with different nucleotides (shown in parentheses). In each experiment, the depleted fraction (fraction names followed by nucleotides in parentheses) was tested in the presence of its untreated complementing fraction (fraction names only). GST-Cdc42-GTPγS beads were used in the visual assay (*a* and *c*), and Cdc42-GTPγS (25 nM) was used in the pyrene actin assay (*b* and *d*).

Table 1 Purification table

Fractionation step	Activity*, units	Protein, mg	Specific activity, units/mg	Recovery, %
Resource Q flow through	32,000	300	107	100
Ammonium sulfate precipitation	16,667	133	125	52
Resource phenyl	15,000	55	273	47
Mono S	4,670	1.8	2,594	15
Superdex-75	2,500	0.9	2,778	8
Mono Q	250	0.2	1,250	0.8

*The activity was estimated based on a visual scoring system. Six minutes after each reaction was started, the sample was evaluated by fluorescence microscopy. The activity was defined as the amount of the rhodamine-labeled actin around the beads, judged by the fluorescence intensity, with an increasing scale from 1 to 5 units. 0 units indicates that there was no localized rhodamine signal.

flow through fraction by using conventional column chromatography and assayed each fraction in the presence of MCAP2. Five additional steps were used sequentially to purify MCAP1 (Table 1). The MCAP1 activity first was precipitated by ammonium sulfate. The precipitate then was resuspended and applied to a hydrophobic interaction column (Resource Phenyl). Fractions from the column with peak activity were pooled and then were applied to a cation exchange column (Mono S). The activity peak from the Mono S column then was subjected to gel filtration chromatography by using a Superdex-75 column. MCAP1 appeared in a major protein peak after the void and contained seven major polypeptides along with some minor contaminants when examined by SDS/PAGE (Fig. 3*a*). To determine whether these proteins were responsible for the activity, the fractions containing peak activity from the gel filtration column were refractionated on another anion exchange column (Mono Q) equilibrated at pH 8.8. The MCAP1 activity profile from the Mono Q column corresponded exactly to the protein profile of the seven polypeptides (Fig. 3*b*). As expected, the activity from the Mono Q column depended on

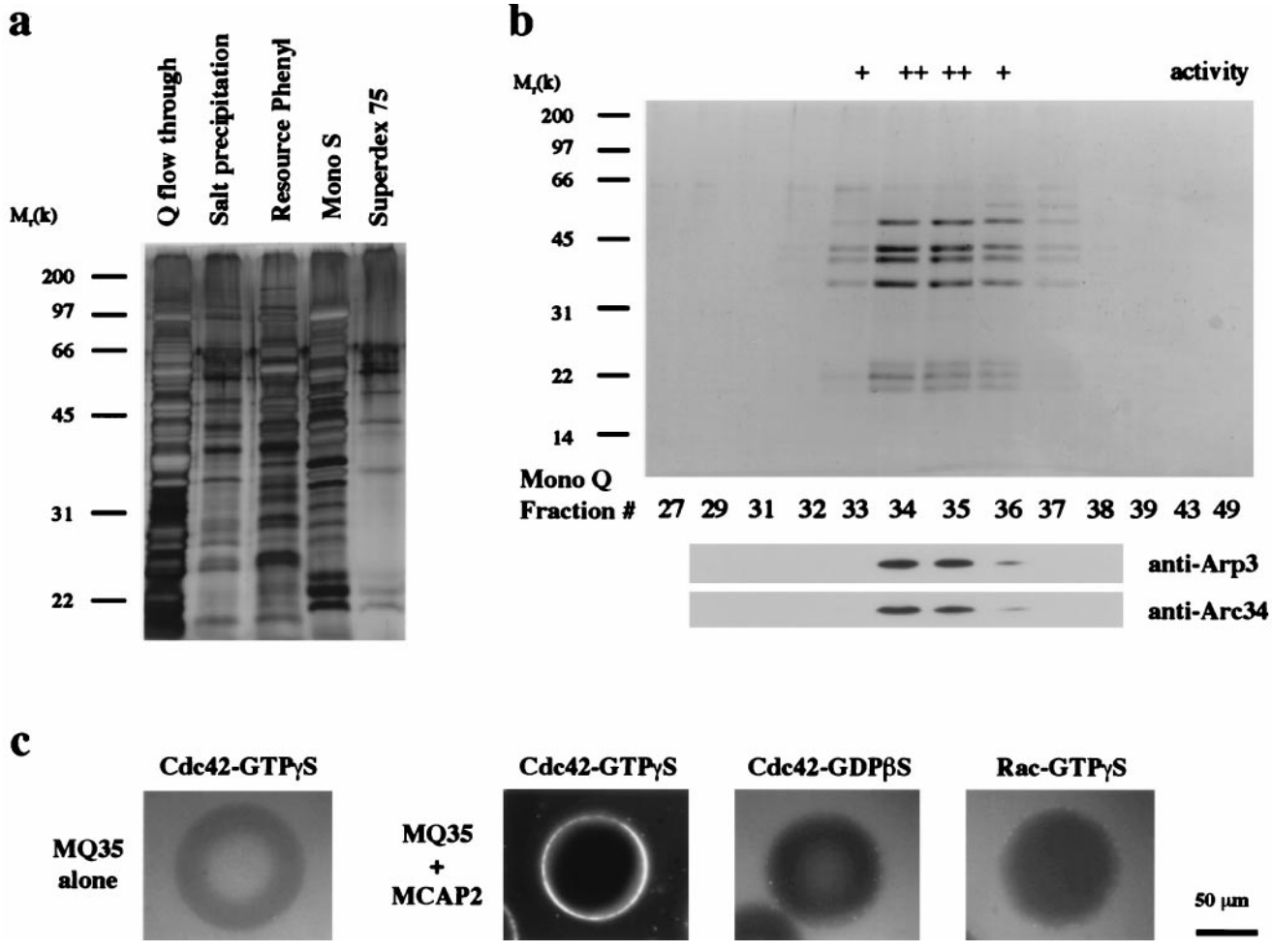

FIG. 3. Purification of MCAP1 from *Xenopus* egg extracts. (*a*) The protein compositions of the active fractions from the first five purification steps are shown on a 12.5% SDS-polyacrylamide gel stained with silver. (*b*) The MCAP1 activity exactly cofractionates with the Arp2/3 complex at the last purification step. Proteins from the Mono Q fractions containing and flanking the active peak were separated by 12.5% SDS/PAGE and either were stained with Gelcode Blue (Pierce) (upper) or were immunoblotted with antibodies against human Arp3 and Arc34 (lower). The activity was estimated based on the fluorescence intensity around the bead on a six-unit scale. (*c*) Analysis of Cdc42-induced actin polymerization in the peak fraction (MQ35, 3 μl) from the Mono Q column in the presence or absence of a MCAP2-containing fraction (3 μl) and different small GTP-binding proteins in the visual assay.

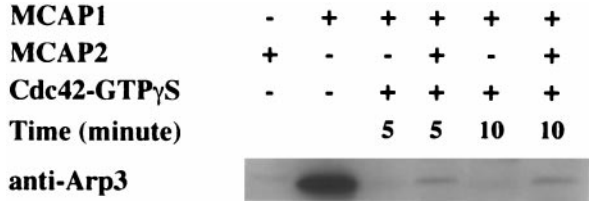

FIG. 4. Association of the Arp2/3 complex with Cdc42 depends on MCAP2. The MCAP1 fraction (11 μl) was incubated with GST-Cdc42-GTPγS beads in the presence or absence of MCAP2 for 5 or 10 minutes. Proteins bound to the beads were analyzed by immunoblotting with the anti-Arp3 antibody. As controls, MCAP1 and MCAP2 (0.5 μl) also were included on the blot.

MCAP2 and was specific for GTPγS-charged Cdc42 (Fig. 3*c*).

The seven polypeptides form a relatively stable complex because they cofractionate on a Superose-6 gel filtration column and on a sucrose-density gradient after sedimentation. The native molecular weight of the complex is 216, calculated from its Stoke's radius (5.2 nm) and sedimentation coefficient (9.5 S). The molecular weights of the polypeptide in the complex estimated by SDS/PAGE are 50, 43, 40, 35, 23, 21, and 19, giving the complex a total mass of 231 kDa, on the assumption that it contains only one of each polypeptide. The polypeptide composition of MCAP1 is extremely similar to the Arp2/3 complex, an evolutionary conserved complex found in humans (20), *Acanthamoeba castellanii* (21), and yeast (22). This identity was confirmed by immunoblotting with antibodies (from Matt Welch, University of California, San Francisco) against human Arp3 and Arc34, two subunits of the complex (20) (Fig. 3*b*).

The Arp2/3 complex was present in the flow through but not the eluate of the Resource Q column, as judged by immunoblotting using antibodies against Arp3 and Arc34 (Fig. 4). It cofractionated with MCAP1 at each subsequent purification step (data not shown). Like MCAP1, the Arp2/3 complex did not bind Cdc42 directly. When the MCAP1 fraction was incubated with GST-Cdc42-GTPγS-containing beads, no association was observed between the Arp2/3 complex and Cdc42 in a spin down assay (Fig. 4). However, the complex could interact with Cdc42 when MCAP2 was included (Fig. 4). Finally, the Arp2/3 complex was unable to support Cdc42-induced actin polymerization in the absence of MCAP2 (Fig. 3*c*). We conclude that the Cdc42-induced actin polymerization requires both the Arp2/3 complex and MCAP2.

DISCUSSION

The discovery of the Arp2/3 complex has provided some insights into the regulation of actin nucleation in cells. The complex was originally isolated from *A. castellanii* extracts on a profilin-affinity column (21) and later was purified as a host protein required for actin polymerization induced by *L. monocytogenes* (23). Biochemical and biophysical analyses have shown that the Arp2/3 complex has filament nucleation, pointed end capping, and filament side binding activities and can organize filaments into branched networks *in vitro* (14, 24). A recent study of ActA, the only *L. monocytogenes* protein required for actin polymerization, raises the possibility that the Arp2/3 complex might be under regulation in cells. In the presence of both purified Arp2/3 complex and ActA, the initial rate of actin polymerization is increased drastically, demonstrating that ActA activates the nucleation activity of the complex (15). This important result strongly points to the presence of analogous cellular mechanisms for controlling actin polymerization. The identification of the Arp2/3 complex in our assay suggests that Cdc42 and MCAP2 might be one example of such cellular mechanisms.

As a molecular switch, Cdc42 interacts with many signaling pathways, potentially allowing cells to integrate signals (25) and regulate actin polymerization in a spatially and temporally restricted way. Indeed, activated Cdc42 is able to remodel actin networks at the cell surface and generate polarized structures like filopodia (2, 3); however, the detailed mechanism by which Cdc42 modulates the actin cytoskeleton has remained obscure. Our results now provide a direct molecular link between Cdc42 and actin polymerization and indicate that, at least in the *Xenopus* system, the activation of the Arp2/3 complex is a critical step. The recent finding that Cdc42 increases the number of free barbed ends in neutrophil extracts (26) also suggests that Cdc42 activates a nucleation factor like the Arp2/3 complex. Although the complex is likely to mediate Cdc42-induced actin polymerization in cells, how it is activated by Cdc42 is not clear. Because MCAP2 is required for the interaction of the complex with Cdc42, its identification will be crucial in elucidating the activation mechanism of the Arp2/3 complex. Currently, we are trying to purify MCAP2 from different tissue sources because it is labile and not abundant in *Xenopus* egg extracts.

Based on its *in vitro* activities (14, 24), a "dendritic nucleation" model has been proposed (14) for how the Arp2/3 complex nucleates actin filaments and organizes them into the branched network observed at the leading edge of motile cells (27). Although the complex has been localized to lamellipodia, filopodia, and pseudopodia (20, 21, 28), it is not clear how the complex is activated locally at these sites. Our biochemical data now suggest a general mechanism for such an activation process that generates localized actin polymerization in response to upstream signals (Fig. 5). After it is activated at the cell membrane, presumably involving phosphoinositides and guanine nucleotide exchange factors as second messengers (13), Cdc42 activates the nucleation activity of the Arp2/3 complex at the plasma membrane through MCAP2. Actin filaments start to polymerize from the activated complex. Inactivation of Cdc42 by nucleotide hydrolysis then disrupts its association with the Arp2/3 complex, releasing the nascent filament polymerized from the complex. This nucleotide-

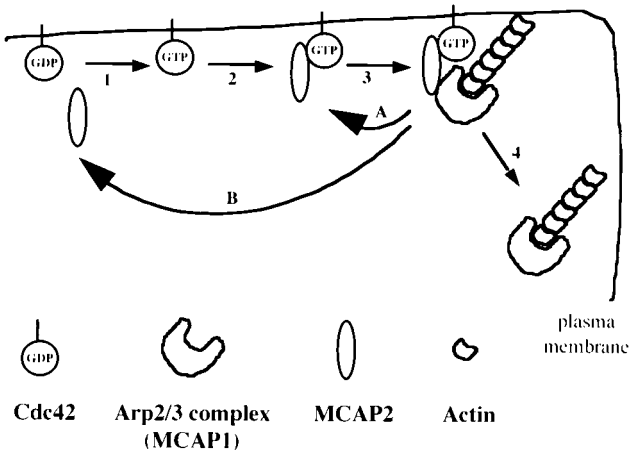

FIG. 5. A general model for the activation of the Arp2/3 complex and the generation of localized actin polymerization by Cdc42 at the leading edge of a cell. Activation of Cdc42 through nucleotide exchange (1) triggered by upstream signal molecules recruits MCAP2 to the cell surface (2), leading to the activation of the Arp2/3 complex and resulting actin polymerization (3). The newly assembled filament then is released (4) because of either the transient association of the Arp2/3 complex with MCAP2 (A) or inactivation of Cdc42 by nucleotide hydrolysis (B). In either case, new filaments will be generated continuously until Cdc42 is inactivated (A) or the upstream signal is turned off (B). Actin filaments are shown to have their barbed ends oriented toward the cell membrane to account for the polarity of filaments observed in cells.

dependent activation and inactivation of Cdc42 could drive a cycle of filament nucleation and release. Alternatively, if the Arp2/3 complex is associated with MCAP2 transiently, activated Cdc42 could allow multiple rounds of filament nucleation before it is inactivated. Because the Arp2/3 complex binds tightly to the pointed end of the nascent filament (14), the released filament may continue to grow until it is capped.

This surface activation model could be the core mechanism for activating actin polymerization by signaling molecules at the plasma membrane. However, generation of complex structures like filopodia must require more than localized actin nucleation. For example, the neuronal Wiskott–Aldrich syndrome protein has been shown to modulate filopodium formation by its actin depolymerization activity (11). Understanding of filopodium formation and other complex processes should require the identification of additional components that modulate filament formation and subsequent organization at different steps.

We thank Kimberly Tolias and Christopher Carpenter for providing the baculoviruses containing recombinant G protein fusion genes and Ann Georgi for expressing these fusion proteins in Sf9 cells. We thank Matt Welch for providing antibodies against Arp3 and Arc34. We thank Lewis Cantley and Tim Mitchison for many helpful discussions and all members of the Kirschner lab for their help and advice during the course of this work. We also thank Jeff Peterson and Ethan Lee for comments on the manuscript. This work was supported by a National Institute of Health grant to M.W.K. (GM26875).

1. Hall, A. (1998) *Science* **279,** 509–514.
2. Nobes, C. D. & Hall, A. (1995) *Cell* **81,** 53–62.
3. Kozma, R., Ahmed, S., Best, A. & Lim, L. (1995) *Mol. Cell. Biol.* **15,** 1942–1952.
4. Johnson, D. I. & Pringle, J. R. (1990) *J. Cell Biol.* **111,** 143–152.
5. Stowers, L., Yelon, D., Berg, L. J. & Chant, J. (1995) *Proc. Natl. Acad. Sci. USA* **92,** 5027–5031.
6. Drechsel, D. N., Hyman, A. A., Hall, A. & Glotzer, M. (1997) *Curr. Biol.* **7,** 12–23.
7. Manser, E., Leung, T., Salihuddin, H., Tan, L. & Lim, L. (1993) *Nature (London)* **363,** 364–367.
8. Manser, E., Leung, T., Salihuddin, H., Zhao, Z. S. & Lim, L. (1994) *Nature (London)* **367,** 40–46.
9. Luo, L., Lee, T., Tsai, L., Tang, G., Jan, L. Y. & Jan, Y. N. (1997) *Proc. Natl. Acad. Sci. USA* **94,** 12963–12968.
10. Symons, M., Derry, J. M., Karlak, B., Jiang, S., Lemahieu, V., Mccormick, F., Francke, U. & Abo, A. (1996) *Cell* **84,** 723–734.
11. Miki, H., Sasaki, T., Takai, Y. & Takenawa, T. (1998) *Nature (London)* **391,** 93–96.
12. Zigmond, S. H., Joyce, M., Borleis, J., Bokoch, G. M. & Devrotes, P. N. (1997) *J. Cell Biol.* **138,** 363–374.
13. Ma, L., Cantley, L. C., Janmey, P. A. & Kirschner, M. W. (1998) *J. Cell Biol.* **140,** 1125–1136.
14. Mullins, R. D., Heuser, J. A. & Pollard, T. D. (1998) *Proc. Natl. Acad. Sci. USA* **95,** 6181–6186.
15. Welch, M. D., Rosenblatt, J., Skoble, J., Portnoy, D. A. & Mitchison, T. J. (1998) *Science* **281,** 105–108.
16. Murray, A. W. (1991) *Methods Cell Biol.* **36,** 581–605.
17. Self, A. J. & Hall, A. (1995) *Methods Enzymol.* **256,** 3–10.
18. Theriot, J. A., Rosenblatt, J., Portnoy, D. A., Goldschmidt-Clermont, P. J. & Mitchison, T. J. (1994) *Cell* **76,** 505–517.
19. Marchand, J. B., Moreau, P., Paoletti, A., Cossart, P., Carlier, M. F. & Pantaloni, D. (1995) *J. Cell Biol.* **130,** 331–343.
20. Welch, M. D., DePace, A. H., Verma, S., Iwamatsu, A. & Mitchison, T. J. (1997) *J. Cell Biol.* **138,** 375–384.
21. Machesky, L. M., Atkinson, S. J., Ampe, C., Vandekerckhove, J. & Pollard, T. D. (1994) *J. Cell Biol.* **127,** 107–115.
22. Winter, D., Podtelejnikov, A. V., Mann, M. & Li, R. (1997) *Curr. Biol.* **7,** 519–529.
23. Welch, M. D., Iwamatsu, A. & Mitchison, T. J. (1997) *Nature (London)* **385,** 265–269.
24. Mullins, R. D., Stafford, W. F. & Pollard, T. D. (1997) *J. Cell Biol.* **136,** 331–343.
25. Van, A. L. & D'Souza, S. C. (1997) *Genes Dev.* **11,** 2295–2322.
26. Zigmond, S. H., Joyce, M., Yang, C., Brown, K., Huang, M. & Pring, M. (1998) *J. Cell Biol.* **142,** 1001–1012.
27. Svitkina, T. M., Verkhovsky, A. B., McQuade, K. M. & Borisy, G. G. (1997) *J. Cell Biol.* **139,** 397–415.
28. Kelleher, J. F., Atkinson, S. J. & Pollard, T. D. (1995) *J. Cell Biol.* **131,** 385–397.